

RACE: RISC-V SoC for En/decryption ACceleration on the Edge for Homomorphic Computation

Zahra Azad ^{*}, Guowei Yan ^{*}, Rashmi Agrawal ^{*}, Daniel Petrisko [†], Michael Taylor [†], Ajay Joshi ^{*}

^{*} Boston University, [†] University of Washington
 {zazad, guowei, rashmi23, joshi}@bu.edu, {petrisko, profmbt}@cs.washington.edu

Abstract—As more and more edge devices connect to the cloud to use its storage and compute capabilities, they bring in security and data privacy concerns. Homomorphic Encryption (HE) is a promising solution to maintain data privacy by enabling computations on the encrypted user data in the cloud. While there has been lot of work on accelerating HE computation in the cloud, little attention has been paid to optimize the en/decryption on the edge. Therefore, in this paper, we present RACE, a custom-designed area- and energy-efficient SoC for en/decryption of data for HE. Owing to similar operations in en/decryption, RACE unifies the en/decryption datapath to save area. RACE efficiently exploits techniques like memory reuse and data reordering to utilize minimal amount of on-chip memory. We evaluate RACE using a complete RTL design containing a RISC-V processor and our unified accelerator. Our analysis shows that, for the end-to-end en/decryption, using RACE leads to, on average, $48\times$ to $39729\times$ (for a wide range of security parameters) more energy-efficient solution than purely using a processor.

I. INTRODUCTION

Over the last decade, Homomorphic Encryption (HE) has emerged as one of the key techniques to perform privacy-preserving computations. Edge devices (having energy and area constraints) can therefore leverage cloud services to compute on private user data using HE. Figure 1 shows an example use case for HE-based computing where a user captures a picture/video using an edge device, pre-processes it, encrypts it, and then sends it to the cloud for further processing. The cloud operates on the data in its encrypted form and sends the encrypted result back to the user, and only the user can decrypt the result.

Several recent works have focused on accelerating the HE operations on the cloud through algorithmic optimizations for CPU [1], [2], GPU [3], [4], and custom hardware accelerators [5]–[9]. All these works make an implicit assumption that the edge-side operations, including encryption and decryption (en/decryption), encoding and decoding (en/decoding), and error sampling are trivial and do not need to be accelerated. However, these edge-side operations are not trivial, and have high compute and memory requirements. SEAL-Embedded is the first HE library targeted for embedded devices, which employs several computational and algorithmic optimizations to achieve memory efficient en/decoding and en/decryption on edge devices [10]. They target Cheon, Kim, Kim and Song (CKKS) [11] HE scheme as it operates on floating-point data, which enables computing on the variety of data captured by the edge device sensors.

However, the memory efficient implementation of the library has performance bottlenecks (e.g., inefficient modular arithmetic implementation) and is still not practical. For example, if we were to encrypt video captured by a QQVGA cameras operating at a low resolution of 120×160 pixels using memory-efficient SEAL-Embedded library (running at 1 GHz on a RISC-V core like BlackParrot [12] for polynomial degree of $N = 4096$ and three 30-bit primes), we cannot encrypt even one frame per second (more details in Section V). Typically surveillance cameras and mobile platforms (forming the ‘Internet of Video Things’) have an average industry

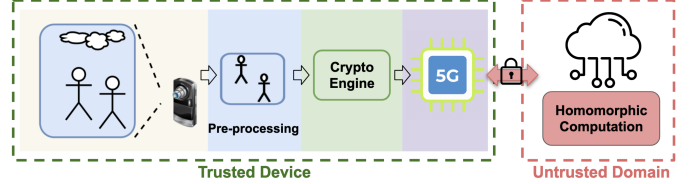


Fig. 1: Steps taken to transfer encrypted video frames to the cloud.

frame rate of 15 and 30 frames per second [13]. One could use a more powerful processor, but then the resulting power consumption would be higher which would not be sustainable in a typical edge device.

The key bottleneck of the edge-side operations is the en/decryption operation, where in the main bottleneck is the **Number Theoretic Transform (NTT) operation**. Several prior works have accelerated the NTT operation in the context of Post Quantum Cryptography (PQC) [14]–[19]. However, the parameters used by these works are much smaller (polynomial degree $N \leq 2^{10}$ and coefficient bit width $\log Q \leq 24$) than the required parameters for a practical HE application ($N > 2^{12}$ and $\log Q > 109$). None of these NTT accelerators focus on designing an area and energy-efficient solution for en/decryption to support HE-based computing. Su et al., proposed an FPGA [20] accelerator for en/decryption targeting Brakerski-Gentry-Vaikuntanathan (BGV) HE scheme [21], but it supports small security parameters ($N = 2^7$). Similarly, Yoon et al., also proposed an ASIC based en/decryption accelerator [22], but it is also evaluated only for small security parameters ($N = 2^4$).

In this work, we present **RACE: a custom-designed area- and energy-efficient RISC-V System-on-Chip (SoC) for en/decryption of the data on the edge**. Encryption and decryption perform similar operations (polynomial addition and multiplication), and so we propose a unified accelerator, where the encryption and decryption operations share the datapath. To reduce SRAM area in RACE we architect it such that it requires memory that is large enough to only store two polynomials. This memory is reused over time to store inputs, outputs, and intermediate values. We propose a novel data reordering scheme for NTT so that RACE only needs single port (1RW) SRAM banks, which further reduces area in contrast with prior works [14]–[18], [23] that need dual port (1R1W) SRAM banks. We interface our accelerator with BlackParrot [12] to design a complete SoC. We provide an end-to-end evaluation of our SoC when performing the en/decryption operation using the accelerator and the remaining operations on the BlackParrot processor. We compare our SoC against a BlackParrot only (BP only) system where all operations are performed on the BlackParrot processor. For both designs we leverage the SEAL-Embedded library. The main contributions of our work are as follows:

- We profile SEAL-Embedded based edge-side operations for the CKKS scheme on BlackParrot, for different N and $\log Q$ pairs to identify the performance bottlenecks.

- Based on the profiling results, we architect RACE, an area- and energy-efficient SoC to accelerate the en/decryption operations. We use a shared data path for the en/decryption operations, and memory reuse and data reorder techniques to architect an efficient accelerator design.
- We interface the accelerator with BlackParrot and evaluate the performance and energy efficiency of RACE when performing end-to-end en/decryption operations.

For the end-to-end encryption and decryption operation, RACE decreases Energy Delay Product (EDP) by $38.67\text{-}75701.92\times$ and $57.93\text{-}3756.25\times$, respectively, compared to the ‘BP only’ system.

II. PRELIMINARIES

A. The CKKS Scheme: En/Decryption Operations

The CKKS HE scheme can efficiently perform computations on encrypted real numbers. The native plaintext data-type in CKKS scheme is a vector of length $N/2$ where each element is chosen from \mathbb{C} , the field of complex numbers. The encoding operation takes as input this $N/2$ -dimensional vector and returns an integer polynomial $m(X)$. Encryption of the polynomial $m(X)$ under the public key pk generates a ciphertext ct by computing the following equations:

$$c_0 = \mu \cdot pk_0 + m + e_0, \quad (1)$$

$$c_1 = \mu \cdot pk_1 + e_1 \quad (2)$$

Here, μ is a uniformly sampled polynomial, and e_0 and e_1 are two polynomials sampled from a discrete Gaussian noise sampler. The coefficients in both the polynomials (c_0, c_1) are elements of \mathbb{Z}_Q , where Q is typically on the order of thousands of bits to account for the noise growth. Therefore, to compute on such large operands efficiently, the CKKS scheme supports the use of Residue Number System (RNS) (also known as the Chinese Remainder Theorem (CRT) representation). Using this approach, each number is represented modulo $Q = \prod_{i=1}^{\ell} q_i$, where each q_i is a prime number. We can represent $x \in \mathbb{Z}_Q$ as a length- ℓ vector of scalars $[x]_B = (x_1, x_2, \dots, x_\ell)$, where $x_i \equiv x \pmod{q_i}$. We refer to each x_i as a *limb* of x . The ciphertext is decrypted to obtain the original message back using the following equation:

$$m = c_0 + c_1 \cdot s \pmod{q_\ell} \quad (3)$$

Here s is the secret key. Using RNS, both en/decryption can be performed with respect to a smaller modulus q_i instead of a large modulus Q .

Video Frame Encryption Example: Considering our example of video frame encryption, using Quarter Quarter VGA (QQVGA) frame resolution, the frame size is 120×160 pixels. If this frame is in grey scale, the frame size will be $120 \times 160 \times 8 = 153,600$ bits = 19.2 KB. With $N = 4096$ and $\log q = 30$ bits, we can encode $N/2 \times \log q = 2048 \times 30 = 61,440$ bits in a single ciphertext, which implies that a single frame will be encoded and encrypted within 3 ciphertexts and will have a total size of 327 KB.

B. BlackParrot: RISC-V Multicore

BlackParrot is an agile open-source RISC-V multi-core processor for accelerator SoCs [12]. It implements the RISC-V RV64G architecture and is designed as a scalable, heterogeneously tiled micro-architecture with a configurable number of tiles. BlackParrot provides a robust and scalable end-to-end framework for accelerator integration, which simplifies interfacing both coherent and streaming accelerators, and the offloading of parts of the user application from the processor to the accelerator. This framework provides hardware implementation of streaming and coherent accelerator tiles in SystemVerilog and

helps accelerator designers and system architects to evaluate their accelerator related ideas and evaluate the end-to-end application time.

III. RELATED WORK

One of the key works in the area of accelerating edge-side operations for HE is the Microsoft SEAL-embedded library [10], which focuses on reducing the memory requirement for en/decoding and en/decryption operations. It uses RNS partitioning, data type compression, memory pooling and reuse to reduce the memory consumption. However, this software-based implementation of HE encryption is still slow and not efficient for real-time applications. As mentioned earlier, for a video application with QQVGA resolution, SEAL-embedded fails to encrypt even one frame per second.

There are few works focusing on accelerating en/decryption for HE [20], [22]. Su et al. [20] present an FPGA-based accelerator, but it is for the BGV HE scheme as against the CKKS scheme that we support. Although their accelerator can be extended to larger polynomial degrees to support higher security levels, in its current form it only supports small parameters ($N = 128$, $\log Q = 27$), which are impractical for HE computation. The authors have left the support for larger parameters as part of the future work. Moreover, the accelerator is mainly optimized for higher performance and throughput, and not for area/energy efficiency. Yoon et al. [22] present an ASIC-based en/decryption accelerator for HE operations. The accelerator is again evaluated for small $N = 16$ only. It needs large buffers to store the in/outputs and the pre-computed twiddle factors, increasing the memory area.

In our work, we can perform en/decryption for any practical security parameters. We share the datapath, adopt memory reuse and data reordering strategies, and compute all the twiddle factors on-the-fly to enable efficient en/decryption operations.

IV. RACE SYSTEM DESIGN AND FUNCTIONALITY

In this section, we first discuss the dataflow for en/decryption and then present the overall architecture of RACE, a complete SoC (see Figure 2) that contains a unified accelerator to efficiently perform en/decryption operations on the edge.

A. Dataflow for Encryption and Decryption

Figure 3(a) shows the encryption dataflow, which is described by Equation (1) and (2). Both the equations perform polynomial addition and multiplication operations to compute the ciphertext. While polynomial addition is straight-forward, NTT is commonly used to speedup polynomial multiplication. We split the operations on $(pk_0, \mu, m + e_0)$ to calculate c_0 and operations on (pk_1, μ, e_1) to calculate c_1 into two ‘half-encryption’ operations. Thus, every encryption operation calls the accelerator twice, once for c_0 half-encryption and once for c_1 half-encryption. Figure 3(b) shows the dataflow for the decryption operation. The decryption operation follows Equation (3) and accepts inputs in NTT format. At a high-level, the half-encryption and decryption operations perform the same underlying operations, just in a different order. Hence, we share the datapath and control logic of the accelerator between the encryption and decryption to lower the accelerator area (see Figure 3(c)).

B. RACE System View

RACE SoC consists of a single-core configuration of BlackParrot and an en/decryption accelerator. We interface the en/decryption accelerator with BlackParrot as a streaming accelerator because it needs a large amount of input and output data transfers (tens of

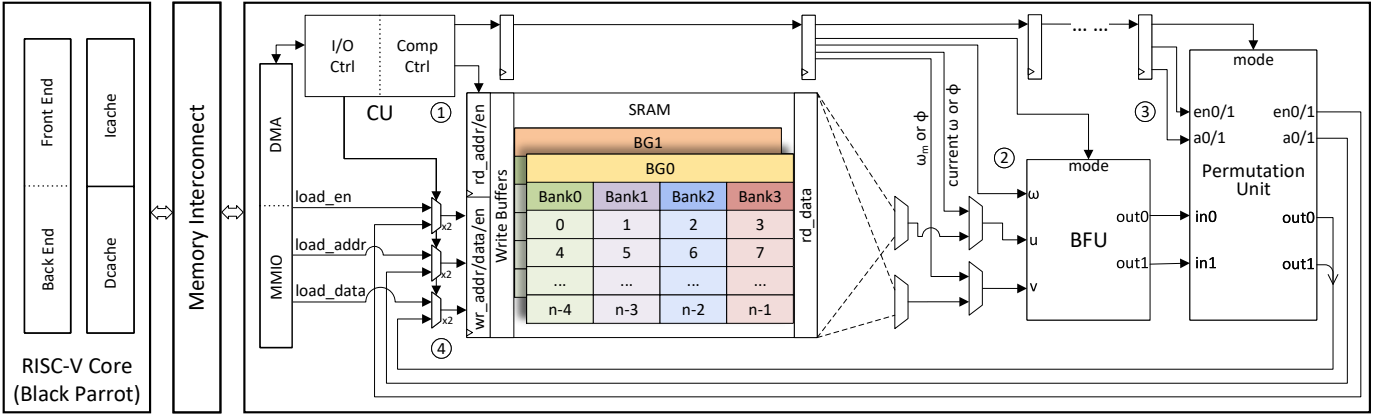


Fig. 2: System-level view of RACE, a RISC-V based SoC for accelerating encryption and decryption operation on the edge for supporting homomorphic operations in the cloud.

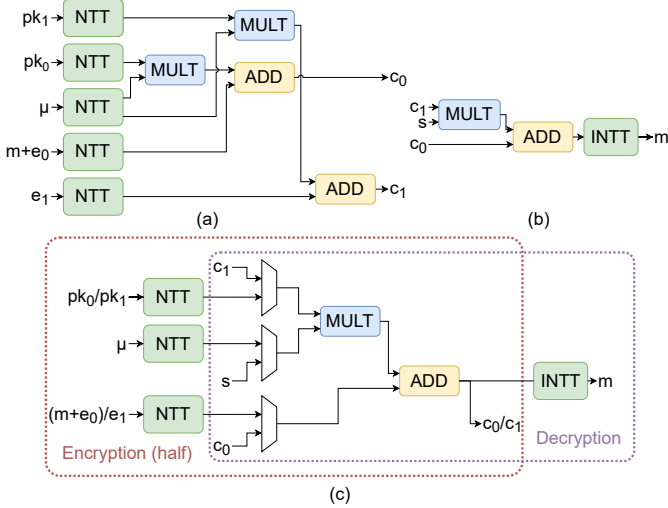


Fig. 3: (a) Encryption dataflow. (b) Decryption dataflow. (c) Unified en/decryption dataflow. In the unified dataflow, encryption and decryption share the datapath and the control logic.

KBs). We set up a hardware DMA logic to transfer all the input data from the main memory to the accelerator tile. The required input data includes pk_0 , pk_1 , e_0 , e_1 and μ . Once the accelerator completes en/decryption operation, it sends an interrupt to the BlackParrot core to signal a completion of the operation. Then, the DMA logic transfers the accelerator output data to the main memory that can be read by BlackParrot for further processing.

C. Accelerator Microarchitecture

Figure 2 shows the detailed microarchitecture of our pipelined accelerator. The accelerator consists of SRAM banks that store the in/output and intermediate polynomials. The Butterfly Unit (BFU) is pipelined and is designed to perform NTT, INTT, polynomial addition and multiplication operations that are required by both encryption and decryption operations (see Figure 3). The permutation unit (PU) reorders (more details given later in this section) the output generated by the BFU and writes it back into the SRAM banks. The control unit (CU) generates activation signals for different datapaths corresponding to the different operations.

1) **BFU**: A Butterfly operation (BF) is the building block of NTT/INTT. An NTT/INTT operation consists of $\log_2 N$ stages ($N-1$ is the polynomial degree), and each stage contains $N/2$ BF.

Given a polynomial a , a BF takes its two coefficients (a_i, a_j) as input and computes $(a_i, a_j) = (a_i + \omega \cdot a_j \pmod{q}, a_i - \omega \cdot a_j \pmod{q})$ (refer Algorithm 1 line 13 and 14). Here, ω is the twiddle factor. A degree $N-1$ polynomial requires $N/2$ twiddle factors, where each twiddle factor needs $\log(q)$ bits. To reduce the memory overhead for storing pre-computed twiddle factors, our accelerator computes them on-the-fly within BFU.

BFU is a fully-pipelined module with the throughput of 1 BF per cycle. It contains a modular multiplier where modular reduction operation is performed using a Barrett reduction [24] unit. BFU also has an integer adder and subtractor unit that performs modular reduction using conditional operator. The latency of the pipelined modular multiplier can be tuned through the number of pipeline stages. The multiplier lies on the critical path in the accelerator, and we pipeline the multiplier to reduce the critical path and improve the frequency of the accelerator. As power and area are the primary design goals for embedded devices, all the above computations are performed by sequentially leveraging the pipelined BFU.

2) **SRAM Arrays**: We use the SRAM arrays to store the in/output and intermediate polynomials. We propose two key ideas: memory reuse and memory reorder to minimize the SRAM size requirements.

Memory reuse: For efficient en/decryption computation, all the required polynomials (m , e_0 , e_1 , μ , pk_0 , pk_1 , c_0 , c_1) should be stored in the on-chip memory of the accelerator. However, a single polynomial is usually large and requires large amount of memory. For $N = 2^{14}$, $\log(q) = 30$ we need 480 KB to store all the in/output polynomials. In our memory reuse approach, we manage the en/decryption operations such that at any point of time we need to store at most two polynomials, which require 122 KB space. We divide the on-chip SRAM memory into multiple banks. Each polynomial is stored across multiple banks and those banks together form a group. We have two bank groups i.e., BG0 and BG1 for the two polynomials. These bank groups are used for storing the in/output and intermediate polynomials during en/decryption operation. Figure 4(a) and (b) show how the two bank groups are shared among the various polynomials during encryption and decryption operation, respectively. For example, we perform an in-place NTT/INTT operation that reads the data for polynomial μ from BG0, operates on it, and writes the results back BG0. While computing NTT on the polynomial μ , we load the next input polynomial pk_1 into BG1 in parallel. We perform memory reuse during the modular addition and multiplication operations as well. Both of these operations read inputs from bank groups BG0 and BG1 and write the results

Algorithm 1: NTT_swap4

Input: Polynomial $a(x) \in \mathbb{Z}_q[x]$ in bit-reversed order
Output: $NTT(a(x))$ in normal order

```

1  $m=2$ ;
2 for ( $stage=0; stage < (\log N - 1); stage+=1$ ) do
3    $\omega=1; \omega_m=\omega_n^{2^{\log N - 1 - stage}}; upd\_cnt=1$ ;
4   for ( $j=0; j < m*2; j+=4$ ) do
5     for ( $k=0; k < N; k+=m*4$ ) do
6        $i0=[]; i1=[]$ ;
7       for ( $l=0; l < 4; l+=1$ ) do
8         switch  $l$  do
9           case 0 do  $idx=j+k$ ;
10          case 1 do  $idx=j+k+2$ ;
11          case 2 do  $idx=j+k+m*2$ ;
12          case 3 do  $idx=j+k+m*2+2$ ;
13           $a[idx]=a[idx]+a[idx+1]*\omega \pmod q$ ;
14           $a[idx+1]=a[idx]-a[idx+1]*\omega \pmod q$ ;
15           $i0.append(idx); i1.append(idx+1)$ ;
16          if  $upd\_cnt == N/(2^{stage+1})$  then
17             $\omega=\omega*\omega_m \pmod q$ ;  $upd\_cnt=1$ ;
18          else  $upd\_cnt+=1$ ;
19           $(a[i0[0]], a[i1[0]], a[i0[1]], a[i1[1]],$ 
20            $a[i0[2]], a[i1[2]], a[i0[3]], a[i1[3]]) =$ 
21            $(a[i0[0]], a[i0[1]], a[i0[2]], a[i0[3]],$ 
22            $a[i1[0]], a[i1[1]], a[i1[2]], a[i1[3]])$ 
23    $m = (m == N/4) ? 2 : (m*2)$ ;
24   for ( $i=0; i < N; i+=1$ ) do
25     /* Bit manipulation */
26      $phy\_addr = \{i[\log N - 3:2], i[\log N - 1:\log N - 2], i[1:0]\}$ ;
27      $a\_out[i] = a[phy\_addr]$ ;
28 return  $a\_out$ ;
```

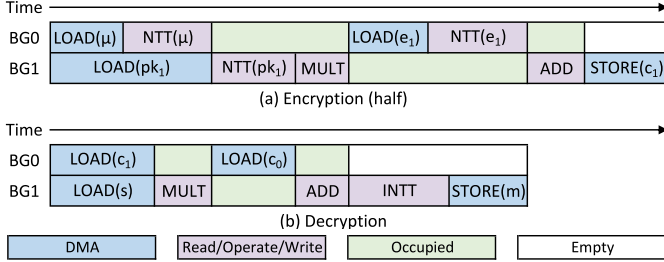


Fig. 4: Memory reuse during (a) encryption and (b) decryption operations. Each BG can store only one polynomial. “Read/Operate/Write” means the bank group is being accessed during the operations. “Occupied” means the bank group stores intermediate results.

back to BG1 only. So we can reuse BG0 for the next operation once the modular addition or multiplication operations are finished. Thus, through memory reuse approach, we can perform en/decryption efficiently using a small memory that stores only two polynomials. **Memory reorder:** A naïve implementation of the NTT algorithm requires 2 read and 2 write port (2R2W) memory bank of size N to achieve two reads and two writes per BF. 2R2W banks are almost $2\times$ larger than 1 read and 1 write port (1R1W) bank. Therefore, just by replacing a single 2R2W bank of size N with two 1R1W banks of size $N/2$ (as long as there are no bank conflicts), we can save half of the memory area. However, the distance between the two inputs of a BF, $(j-i)$, varies across NTT stages. NTT operation iterates through all values from 1 to $N/2$, so there are bank conflicts in certain stages, making this replacement impossible. Existing works reduce the required memory ports from 2R2W to 1R1W by customizing the

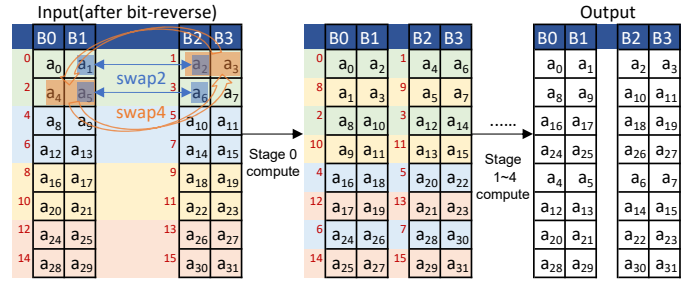


Fig. 5: NTT_swap4 with $N=32$. The red colored numbers before each pair of cells denote the order of BF operations. The consecutive four BFs (2 rows) being reordered are denoted with the same color.

NTT algorithm. For example, to use 1R1W memory banks for an NTT, Roy et al. [25] proposed a memory-efficient NTT algorithm. We call their approach as NTT_swap2 algorithm. This algorithm avoids the bank conflicts (two 1R1W banks) by reordering the output of the two consecutive BF operations. This is to ensure that the pair of inputs needed by BF operation in the next stage resides in different banks.

While the use of 1R1W memory bank saves half the memory area, it is still not efficient. We propose to replace the two 1R1W banks of size $N/2$ with four 1 read/write port (1RW) banks of size $N/4$ to reduce memory area even further. A 1RW bank is $2\times$ smaller than a 1R1W bank. However, this results in newer bank conflicts that cannot be resolved by the existing NTT_swap2 algorithm. If the same bank receives both read and write requests at the same time, we need to have a write buffer that stores the write requests and waits until there are no incoming reads to opportunistically write back the results. The size of the write buffer depends on the number of cycles where the bank is continuously read and written. If there are $N/4$ continuous read and write accesses to the same bank in one particular stage, then the write buffer needs to be the same size as the banks ($N/4$) to store all the write requests that are overlapping with the read requests to the same bank. To avoid the overhead of this large write buffers, we propose a new NTT algorithm called NTT_swap4 (refer Algorithm 1).

On top of NTT_swap2 i.e., reordering the outputs of two BF operations, NTT_swap4 further reorders the output of four consecutive BFs (Figure 5). This is to make sure that not only the two inputs of all BF operations are stored in different banks (NTT_swap2), but also the inputs of consecutive BFs are stored in different banks (NTT_swap4). In this case, the same bank is not continuously accessed and the write buffer can write back the results immediately in the next cycle. Hence, the write buffer can be as small as one element wide ($\log q$), saving further area. Figure 5 shows an example of NTT_swap4 scheme for $N=32$. The numbers (in red) before each pair of cells denote the order of BF operations. For example, in stage 0, the first four BFs access the following pairs: $(a_0, a_1), (a_2, a_3), (a_4, a_5), (a_6, a_7)$. However, stage 1 expects elements in the order of $(a_0, a_2), (a_4, a_6), (a_1, a_3), (a_5, a_7)$. So we reorder the outputs of stage 0 to the order expected by stage 1 to make sure that the consecutive BFs in stage 1 do not access the same banks for reads and writes (refer Algorithm 1 line 19). We use a PU to perform this reordering.

3) **Permutation Unit:** The PU consists of a reordering logic and a small register array to store 8 pairs of BF outputs. Reordering logic starts by writing the two outputs of a BF operation along with their addresses sequentially to the register array in each cycle. After there are eight elements in the register array i.e., four pair of BFU outputs, the reordering logic will first send out the elements stored in even registers and then the elements in odd registers (see memory reorder example

in Section IV-C2). This reordering logic works for both NTT and INTT operations. As shown in Figure 2, depending upon the *mode* signal, the PU will be active only during the NTT/INTT computations.

4) *Control Unit*: The CU consists of two components – the computation controller and the I/O controller. The computation controller is an FSM that determines the BFU and PU mode signals depending upon the current operation (NTT/INTT, modular addition and multiplications). It also generates the read/write addresses and enable signals for SRAM accesses. During NTT/INTT operation, the computation controller is also responsible for stalling the BFU pipeline and configuring it to compute the twiddle factors on-the-fly. The I/O controller selects the required set of BFU operations depending on the CPU request type received by the accelerator (encryption or decryption). In addition, it also sets up the DMA unit for the in/output data transfer to/from SRAM arrays based on the current en/decryption step.

V. EVALUATION

A. Methodology

For our analysis, we run all the edge-side operations from the SEAL-Embedded library on the ‘BP only’ system and RACE in bare-metal mode. In the ‘BP only’ system, we perform all operations on the BlackParrot processor. In RACE, we perform the en/decryption operation using the accelerator and the remaining operations on the BlackParrot processor. We modified SEAL-Embedded library to execute en/decryption operations on the accelerator in RACE. For both ‘BP only’ and RACE, we use BlackParrot SoC with a single core configuration (32 KB each of Icache and Dcache) running at 1 GHz. Both ‘BP only’ and RACE are implemented in SystemVerilog and simulated using VCS. The hardware implementation is cycle-accurate and captures the nuances of data movement between all parts of the systems. For power, performance and area evaluation, we use GlobalFoundries 12 nm technology. We synthesize the logic components in both ‘BP only’ and RACE using Synopsys Design Compiler, and use memory compiler for designing the SRAM arrays.

B. Results

Performance: Figure 6 (a) shows the initial setup, encoding, error sampling, DMA, and encryption latency (in clock cycles) for the ‘BP only’ system and RACE for different security parameters (N , $\log Q$). Note that the Y-axis uses a log scale. Similarly, Figure 6 (b) shows the latency breakdown for the initial setup, decode, decrypt and DMA operations. For the ‘BP only’ system, the en/decryption operations take the longest time because they need multiple polynomial multiplications, where the runtime is dominated by NTT/INTT operations. RACE reduces the NTT/INTT execution time by $78.4\times$ for the smallest N (1024) and $121.8\times$ for the largest N (16384). As a result, the encryption time decreases by $62.56\text{--}515.45\times$ ($80.63\text{--}669.56\times$ w/o considering the DMA overhead) and the decryption time decreases by $126.51\text{--}160.9\times$ ($158.14\text{--}201.12\times$ again w/o considering the DMA overhead), which in turn decreases the end-to-end latency by $7.5\text{--}312.1\times$ and $9.3\text{--}69.5\times$, respectively. The end-to-end performance improvement is lower than that of en/decryption alone because all the initial setup, encoding/decoding and error sampling operations take non-trivial amount of time and are performed in the software.

In Figure 6 (a) and (b), we observe that we get a higher performance improvement for the larger N values. This is because for larger N values we need to perform more BF operations within an NTT and INTT, and we accelerate these very BF operations using hardware. Moreover, as $\log Q$ increases, the number of 30-bit co-primes that

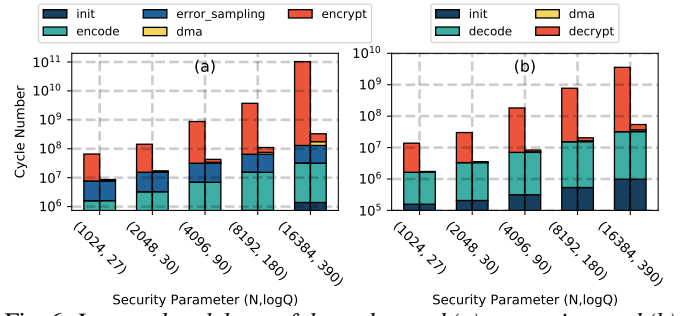


Fig. 6: Latency breakdown of the end-to-end (a) encryption, and (b) decryption for ‘BP only’ (left) and RACE (right). Note that we have used log scale for Y-axis in the plots.

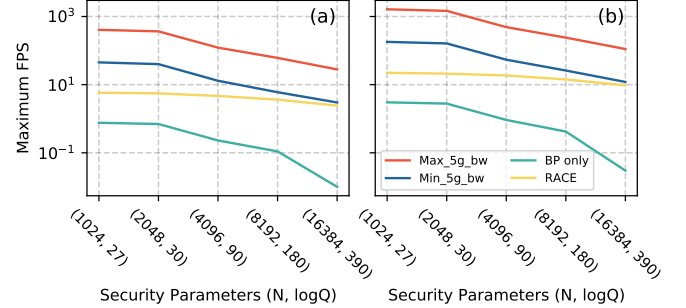


Fig. 7: Maximum supported (a) QVGA and (b) QQVGA frame rate per second (FPS) for mid-band 5G, camera, SEAL-Embedded based encryption, and RACE for different N and $\log(Q)$ values.

we need also increases, which in turn increases the number of times we need to call the encryption and decryption operations (once per co-prime). It is worth noting that for RACE we need to perform DMA operations, but due to the high computational requirements of the en/decryption operations, the DMA overhead is negligible ($<20\%$).

Power/Energy: The total power consumption for an end-to-end en/decryption in the ‘BP only’ system is 27.19 mW, out of which the SRAM power consumption is $41.49\% = 11.4$ mW and the digital logic consumes the rest of the power. Overall, the power consumption of RACE is about 25-28% (for a range of security parameters) higher than the ‘BP only’ system for both end-to-end encryption and decryption procedures. The increase in the power consumption is due to 41.92-43.55% power increase in the digital logic and 3.36–7.81% power increase in the SRAM.

Table I shows the energy consumed in the end-to-end encryption and decryption procedures for different (N , $\log Q$) values when using ‘BP only’ and RACE. Overall, RACE consumes $5.07\text{--}242.5\times$ lower energy when running an end-to-end encryption procedure and $6.2\text{--}54.02\times$ lower energy when running an end-to-end decryption procedure as compared to the ‘BP only’ system. This is because the performance of RACE is up to $312.1\times$ and $69.5\times$ higher for the end-to-end encryption and decryption procedures, but its power overhead is very small. As discussed earlier, RACE speedup is higher for larger security parameters, but the power consumption increases by only 3% for the largest N value compared to the smallest one. Hence, as the security parameters (N , $\log Q$) grow, the end-to-end energy saving per en/decryption increases.

Energy Efficiency: We use Energy Delay Product (EDP) metric to compare the energy efficiency of the ‘BP only’ system and RACE (see Table I). Overall, RACE has $38.67\text{--}75701.92\times$ lower EDP when running an end-to-end encryption procedure and $57.93\text{--}3756.25\times$

TABLE I: End-to-end performance, power, area and EDP comparison for the ‘BP only’ system and RACE.

$(N, \log Q)$	‘BP only’ (en/decryption)				RACE (en/decryption)			
	Latency (ms)	Energy (mJ)	EDP (mJ.ms)	Area (μ^2)	Latency (ms)	Energy (mJ)	EDP (mJ.ms)	Area (μ^2)
(1024, 27)	65.57/13.8	1.78/0.06	116.91/5.18	135880.17	8.61/1.48	0.35/6.21	3.02/0.09	156901.15
(2048, 30)	143.26/30.09	3.90/0.10	558.10/24.62	135880.17	18.04/3.12	0.58/7.66	10.16/0.33	163856.05
(4096, 90)	871.48/182.16	23.70/0.26	20652.58/902.29	135880.17	42.94/7.6	1.47/19.03	63.17/1.98	175639.99
(8192, 130)	3716.09/774.22	101.05/0.65	375516.07/16299.99	135880.17	110.28/19.08	3.78/32.18	416.93/12.48	199668.39
(16384, 390)	102665.07/3576.19	2791.76/1.79	2.86×10^8 /347774.18	135880.17	328.94/51.44	11.51/54.02	3786.11/92.59	250913.93

lower EDP when running an end-to-end decryption procedure as compared to the ‘BP only’ system.

Area: Overall, RACE area is 15% (smallest N) to 84% (largest N) larger than the ‘BP only’ system area. SRAMs occupy (75%) of the area in the ‘BP only’ system, and there is 11%-100% increase in the SRAM area in RACE as compared to the ‘BP only’ system. However, note that we reduce the SRAM requirement from 480 KB to 120 KB for the largest N value by employing various techniques discussed in section IV-C2.

Video Application Evaluation: For the video application discussed earlier, Figure 7 shows the maximum frames per second (FPS) that both the ‘BP only’ system and RACE can sustain for different $(N, \log Q)$ values when performing an end-to-end encryption. The encrypted frames are shipped to the cloud using a mid-band 5G network, which offers a balance of speed, capacity, and coverage [26]. As shown in Figure 7a, in the regions with maximum bandwidth, mid-band 5G network can transfer up to 111 (QQVGA) and 28 (QVGA) frames per second and in the regions with minimum bandwidth, it can only transfer 12 (QQVGA) and 3 (QVGA) frames per second. The ‘BP only’ system is capable of encrypting up to 3 QVGA FPS for N values smaller than 2048 (refer Figure 7). However, as we increase N to 4096 or larger values, it cannot encrypt even a single frame per second. On the other hand, for QVGA RACE encrypts ~ 20 FPS for small values of N and 10 FPS for the largest N value (16384). For QVGA resolution, the ‘BP only’ system cannot encrypt even one FPS for the smallest N value (1024). However, RACE can encrypt 6 and 3 FPS for the smallest and largest N values, respectively. While RACE can support higher FPS than the ‘BP only’, there is still some headroom in both minimum 5G bandwidth and maximum 5G bandwidth cases. Therefore, as part of the future work, we plan to accelerate the en/decoding and the error sampling operations to fully utilize the frame transfer rate that can be sustained by the mid-band 5G network.

VI. CONCLUSION

In this work, we present RACE, a RISC-V based SoC for en/decryption acceleration on the edge to support HE operations in the cloud. RACE implements several optimizations that enable high performance, and area- and energy-efficient end-to-end en/decryption operations. Our analyses show that compared to the ‘BP only’ system, RACE has higher performance and lower energy consumption. As a result, overall RACE is more energy efficient than the ‘BP only’ system, and has 38.67 - $75701.92 \times$ lower EDP when running an end-to-end encryption procedure and 57.93 - $3756.25 \times$ lower EDP when running an end-to-end decryption procedure.

policies or endorsements, either expressed or implied, of Air Force

VII. ACKNOWLEDGMENT

This material is based on research sponsored by Air Force Research Laboratory (AFRL) and Defense Advanced Research Projects Agency (DARPA) under agreement number FA8650-18-2-7856. The views and conclusions contained herein are those of the authors and should not be interpreted as necessarily representing the official

Research Laboratory (AFRL) and Defense Advanced Research Projects Agency (DARPA) or the U.S. Government.

REFERENCES

- [1] W. Jung *et al.*, “HEAAN Demystified: Accelerating Fully Homomorphic Encryption Through Architecture-centric Analysis and Optimization,” 3 2020. [Online]. Available: <http://arxiv.org/abs/2003.04510>
- [2] C. Bootland *et al.*, “Efficiently Processing Complex-Valued Data in Homomorphic Encryption,” *Journal of Mathematical Cryptology*, vol. 14, pp. 55–65, 2020.
- [3] A. A. Badawi *et al.*, “Multi-GPU Design and Performance Evaluation of Homomorphic Encryption on GPU Clusters,” *IEEE TPDS*, vol. 32, no. 2, pp. 379–391, 2021.
- [4] N. Gupta *et al.*, “PQC Acceleration Using GPUs: FrodoKEM, NewHope, and Kyber,” *IEEE TPDS*, vol. 32, no. 3, pp. 575–586, 2021.
- [5] W. Wang *et al.*, “VLSI Design of a Large-Number Multiplier for Fully Homomorphic Encryption,” *IEEE TVLSI*, vol. 22, no. 9, pp. 1879–1887, 2014.
- [6] D. B. Cousins *et al.*, “Designing an FPGA-Accelerated Homomorphic Encryption Co-Processor,” *IEEE TETC*, vol. 5, no. 2, pp. 193–206, 2017.
- [7] D. Reis *et al.*, “Computing-in-Memory for Performance and Energy-Efficient Homomorphic Encryption,” *IEEE TVLSI*, vol. 28, no. 11, pp. 2300–2313, 2020.
- [8] F. Turan *et al.*, “HEAWS: An Accelerator for Homomorphic Encryption on the Amazon AWS FPGA,” *IEEE TC*, vol. 69, no. 4, pp. 1185–1196, 2020.
- [9] M. S. Riaz *et al.*, “HEAX: An Architecture for Computing on Encrypted Data,” *Proc. ASPLOS*, 2020, p. 1295–1309.
- [10] D. Natarajan *et al.*, “SEAL-Embedded: A Homomorphic Encryption Library for the Internet of Things,” *IACR CHES*, vol. 2021, no. 3, pp. 756–779, 2021.
- [11] J. H. Cheon *et al.*, “Homomorphic encryption for arithmetic of approximate numbers,” in *Advances in Cryptology – ASIACRYPT 2017*, Cham, pp. 409–437.
- [12] D. Petrisko *et al.*, “BlackParrot: An Agile Open-Source RISC-V Multicore for Accelerator SoCs,” *IEEE Micro*, vol. 40, no. 4, pp. 93–102, 2020.
- [13] M. A. Usman *et al.*, “An intrusion oriented heuristic for efficient resource management in end-to-end wireless video surveillance systems,” in *Proc. IEEE Annual CCNC*, 2018, pp. 1–6.
- [14] P. Nannipieri *et al.*, “A RISC-V Post Quantum Cryptography Instruction Set Extension for Number Theoretic Transform to Speed-Up CRYSTALS Algorithms,” *IEEE Access*, vol. 9, pp. 150 798–150 808, 2021.
- [15] C. Li *et al.*, “A high speed NTT accelerator for lattice-based cryptography,” in *Proc. CISCE*, IEEE, 2021, pp. 85–89.
- [16] X. Chen *et al.*, “CFNTT: Scalable Radix-2/4 NTT Multiplication Architecture with an Efficient Conflict-free Memory Mapping Scheme,” *IACR CHES*, vol. 2022, pp. 94–126, 2022.
- [17] P. Duong-Ngoc *et al.*, “Configurable Butterfly Unit Architecture for NTT/INTT in Homomorphic Encryption,” in *Proc. ISOC*, 2021, pp. 345–346.
- [18] G. Xin *et al.*, “VPQC: A domain-specific vector processor for post-quantum cryptography based on RISC-V architecture,” *IEEE TCAS-I*, vol. 67, no. 8, pp. 2672–2684, 2020.
- [19] U. Banerjee *et al.*, “Sapphire: A configurable crypto-processor for post-quantum lattice-based protocols,” *arXiv preprint arXiv:1910.07557*, 2019.
- [20] Y. Su *et al.*, “FPGA-based hardware accelerator for leveled ring-LWE fully homomorphic encryption,” *IEEE Access*, vol. 8, pp. 168 008–168 025, 2020.
- [21] C. Gentry *et al.*, “Ring switching in BGV-style homomorphic encryption,” in *Proc. ICSCN*, Springer, 2012, pp. 19–37.
- [22] I. Yoon *et al.*, “A 55nm 50nJ/encode 13nJ/decode Homomorphic Encryption Crypto-Engine for IoT Nodes to Enable Secure Computation on Encrypted Data,” in *Proc. CICC*, 2019, pp. 1–4.
- [23] A. C. Mert *et al.*, “A flexible and scalable NTT hardware: Applications from homomorphically encrypted deep learning to post-quantum cryptography,” in *Proc. DATE*, 2020, pp. 346–351.
- [24] P. Barrett, “Implementing the Rivest Shamir and Adleman public key encryption algorithm on a standard digital signal processor,” in *Conference on the Theory and Application of Cryptographic Techniques*. Springer, 1986, pp. 311–323.
- [25] S. S. Roy *et al.*, “Compact Ring-LWE Cryptoprocessor,” pp. 371–391, 2014. [Online]. Available: http://link.springer.com/10.1007/978-3-662-44709-3_21
- [26] S. R. Thummalur *et al.*, “Four-Port MIMO Cognitive Radio System for Midband 5G Applications,” *IEEE TAP*, vol. 67, no. 8, pp. 5634–5645, 2019.